Chemical Structure and Orientation of Ethylene on Si(114)−(2×1)/c(2×2)

ARTICLE *in* THE JOURNAL OF PHYSICAL CHEMISTRY B · MAY 2006

Impact Factor: 3.3 · DOI: 10.1021/jp055599+ · Source: PubMed

Chemical Structure and Orientation of Ethylene on Si(114)−(2×1)/c(2×2)

D. E. Barlow, S. C. Erwin, A. R. Laracuente, L. J. Whitman, and J. N. Russell, Jr.*

Naval Research Laboratory, Chemistry Division, 4555 Overlook Avenue, SW, Washington, D.C. 20375-5342

Received: September 30, 2005; In Final Form: January 23, 2006

The basic chemical structure and orientation of ethylene chemisorbed on Si(114)−(2×1) at submonolayer coverage is characterized in ultrahigh vacuum using transmission Fourier transform infrared (FTIR) spectroscopy. The spectra are consistent with di-sigma bonding of ethylene to the surface with a preferential molecular orientation over macroscopic lengths. These results are supported by density functional theory (DFT) calculations of vibrational frequencies for optimized ethylene−Si(114) structures occupying the dimer and rebonded atom surface sites. A detailed analysis of the strong angular and polarization dependence of the C−H stretching mode intensities is also consistent with the adsorption structures identified by DFT, indicating that ethylene chemisorbs with the C−C bond axis parallel to the structural rows oriented along the [$\bar{1}$10] direction on the Si(114)−(2×1) surface. The results indicate that the unique structure of this surface makes it an excellent template for elucidating relationships between surface structure and organic reaction mechanisms on silicon.

Introduction

Methods and chemistries to covalently attach organic molecules to single-crystal semiconductor surfaces in ultrahigh vacuum (UHV) have been the subject of considerable interest over the past several years.[1−4] A primary motivation has been the development of methods to incorporate functional organic nanostructures onto semiconductor substrates for electronic and optoelectronic device applications. Most work has been performed on Si(001)−(2×1) because of its technological importance and ease of preparation in UHV. In addition, this surface has a simple surface reconstruction, with a rectangular unit cell of Si surface dimers that is conducive to engineering self-assembled nanostructures.

Although a number of the high index Si crystal faces form stable, planar, reconstructed surfaces, including Si(113), (114), and (5 5 12) in the regime between (001) and (111),[5] to our knowledge, little consideration has been given to these surfaces as substrates for organic molecular chemisorption and self-assembly. These surfaces have properties that make them interesting for such studies, including a variety of surface structures beyond dimers, and often a "single domain"-like arrangement of those structures along one crystallographic direction.[5] It may thus be possible to form orientationally aligned chemisorbed organic monolayers on such surfaces. Aligned chemisorption has been previously demonstrated for ethylene and cyclopentene adsorbed on single-domain vicinal Si(001) (where all steps are double-height and therefore all the dimer rows have the same orientation).[6,7] The high-index surfaces are potentially valuable templates for studying structure-specific, surface-mediated organic self-assembly of molecular nanostructures.

Si(114) is a potentially interesting high-index substrate for organic chemisorption as a logical progression from prior studies on stepped, single-domain, vicinal Si(001) surfaces. Oriented 19.5° from (001) toward (111), the (114) plane is the most vicinal surface to maintain a planar (001)-like terrace-plus-step structure.[5] Although more complex than Si(001)−(2×1),[8,9] the clean Si(114) surface reconstruction includes only two additional structural elements in addition to the dimer row. Moreover, the surface can be monohydride terminated with little change in the surface structure,[10] suggesting that ordered chemisorbed monolayers might be possible despite the presence of multiple potential chemisorption geometries. As displayed in Figure 1, the Si(114)−(2×1) surface consists of periodic rows of rebonded (001)-like "B-type" double-layer steps, tetramers, and (001)-like dimers. This reconstruction, which has a calculated surface energy very close to that of Si(001)−(2×1), results from a unique balance between surface-stress relief and dangling-bond reduction.[8] Note that the rows are parallel to the [$\bar{1}$10] direction and maintain this orientation over the entire sample. Both c(2×2) and (2×1) local symmetries occur, delineated by a simple shift of the dimers by one lattice constant along the row but maintaining the structure within each row.[8,11]

The Si(114)−(2×1)/c(2×2) structures exhibit a variety of bonding characteristics, which should show interesting reactivity with organic adsorbates. Dimers have pi-bonding character like those on Si(001)−(2×1), although they are predicted to be less buckled.[8,9,12] The rebonded atoms periodically buckle along each row, an effect clearly observed by scanning tunneling microscopy (STM) because the buckling is static at room temperature.[8] As with dimers, buckling of the rebonded atoms is accompanied by charge transfer from the "down" atom to the adjacent "up" atom.[3,8,9] The tetramer sites, unique to high index silicon surfaces, are each composed of a (001)-like dimer bonded to two nonrebonded step atoms. Both experiment (STM) and theory observe π-bonding states between the adjacent dimer and nonrebonded step atoms, characteristic of a double bond.[8,9] In analogy to molecular bonding, dimers resemble silenes and tetramers resemble disilenes, as depicted by the double bonds shown in Figure 1.

As an initial investigation into the organic functionalization of Si(114), we identify the chemical structure and orientation of chemisorbed ethylene on Si(114)−(2×1) using transmission FTIR spectroscopy[13] and density functional theory (DFT).

* Corresponding author. E-mail: john.russell@nrl.navy.mil.

10.1021/jp055599+ CCC: $33.50
Published on Web 03/16/2006

Report Documentation Page

Form Approved
OMB No. 0704-0188

1. REPORT DATE	2. REPORT TYPE	3. DATES COVERED
SEP 2005		**00-00-2005 to 00-00-2005**

4. TITLE AND SUBTITLE	5a. CONTRACT NUMBER
Chemical Structure and Orientation of Ethylene on Si(114)-(2x1)/c(2x2)	5b. GRANT NUMBER
	5c. PROGRAM ELEMENT NUMBER
6. AUTHOR(S)	5d. PROJECT NUMBER
	5e. TASK NUMBER
	5f. WORK UNIT NUMBER
7. PERFORMING ORGANIZATION NAME(S) AND ADDRESS(ES) **Naval Research Laboratory,Chemistry Division,4555 Overlook Avenue SW,Washington,DC,20375**	8. PERFORMING ORGANIZATION REPORT NUMBER
9. SPONSORING/MONITORING AGENCY NAME(S) AND ADDRESS(ES)	10. SPONSOR/MONITOR'S ACRONYM(S)
	11. SPONSOR/MONITOR'S REPORT NUMBER(S)

12. DISTRIBUTION/AVAILABILITY STATEMENT
Approved for public release; distribution unlimited

13. SUPPLEMENTARY NOTES

14. ABSTRACT

15. SUBJECT TERMS

16. SECURITY CLASSIFICATION OF:			17. LIMITATION OF ABSTRACT	18. NUMBER OF PAGES	19a. NAME OF RESPONSIBLE PERSON
a. REPORT	b. ABSTRACT	c. THIS PAGE			
unclassified	**unclassified**	**unclassified**	**Same as Report (SAR)**	**7**	

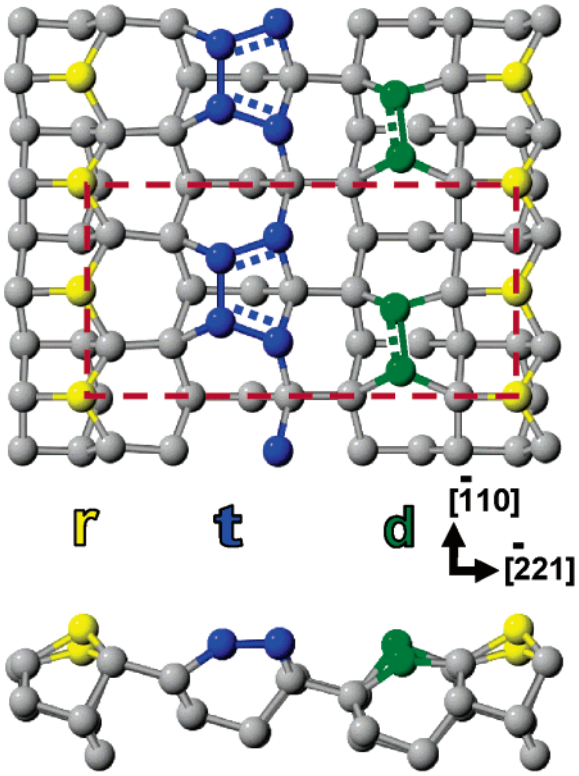

Figure 1. Equilibrium structure of the reconstructed Si(114)−(2×1) surface. The surface is composed of periodic rows of rebonded atoms ("r"), tetramers ("t"), and dimers ("d"). The double bonds (dotted lines) on the dimer and tetramer sites represent a molecular bonding perspective and are shown for the purpose of indicating how these surface sites may react if they behave as molecular species. The (2×1) unit cell, indicated by the dashed lines, measures 7.7 × 16.3 Å^2.

Although FTIR studies of semiconductor surfaces generally use a multiple internal reflection configuration to enhance the surface sensitivity, strong phonon absorption completely attenuates the light below 1500 cm^{-1} for multiple reflections through Si substrates at room temperature. For this reason we optimized the use of single-pass transmission FTIR spectroscopy which—although generating much smaller signals—allows observation of the entire mid-IR region (critical for organics adsorbed on silicon) while providing greater flexibility for acquiring angular and polarization-dependent spectra (important for determining molecular bond orientations).

Experimental Section

Clean and ethylene-dosed Si(114) samples were prepared in a UHV chamber (base pressure ∼1 × 10^{-10} Torr) equipped for characterization by FTIR spectroscopy, low energy electron diffraction (LEED), and Auger spectroscopy. Transmission FTIR spectra were acquired with a nitrogen-purged ThermoNicolet 870 FTIR spectrometer coupled to the UHV chamber through an IR cell equipped with differentially pumped KBr windows. Either an InSb or broadband MCT (MCT-B) liquid nitrogen cooled detector was used. The resolution was set to 8 cm^{-1}, and typically 4000 scans were averaged. A UHV four-axis manipulator was used for sample positioning.

Si(114) samples were cut from double-side polished Si(114) wafers (±0.5°, *p*-type, 1−10 Ω-cm, 1 mm thick; Semiconductor Processing Company) to a size of 9 × 34 mm^2 using a diamond scribe. All samples used for this study were cut with the [1̄10] direction parallel to the 34 mm side of the sample. The samples were mounted on a sample holder similar to that described by Nishino et al.[14] and transferred to the transmission FTIR UHV chamber. After outgassing for 24 h at 500 °C, clean Si(114)−(2×1) surfaces were obtained by resistive heating to 1225 °C using a current-limited power supply. Note that the samples were heated in a separate, attached chamber to prevent silicon deposition on the KBr windows in the IR cell. After the sample cooled to room temperature and achieved thermal equilibrium (∼295 K), background FTIR spectra were obtained with the clean sample in the optical path. The room-temperature sample was then exposed to gas phase (99.98%, Matheson) ethylene by backfilling the chamber and monitoring the pressure with an uncorrected ion gauge. Single beam sample FTIR spectra were then acquired, ratioed against the background, and converted to absorbance. Fourier processing of the interferograms included Happ-Genzel apodization, Mertz phase correction, and two levels of zero filling.[15] This was found to provide the best balance between peak resolution and signal-to-noise for the particular spectra under study. Minor baseline corrections were also applied to the presented spectra. By acquiring the data at 8 cm^{-1} resolution with 1 mm thick Si(114) samples, the interferograms were sufficiently truncated to avoid the appearance of interference fringes in the spectra.[15]

FTIR spectra were acquired in three different configurations. For broad-spectrum studies, spectra were recorded with the sample at 74° from normal incidence (Si Brewster angle) using unpolarized incident light and an MCT-B detector. For studies of the molecular orientation and symmetry, spectra were recorded with an InSb detector using polarized incident light and the sample at normal incidence. The light was polarized with a wire grid polarizer located at the entrance window of the chamber and configured either parallel or perpendicular to the [1̄10] direction of the substrate.

Theoretical

Adsorption energies and harmonic vibrational frequencies for C_2H_4 on Si(114) were calculated from DFT in the generalized-gradient approximation,[16] using the projector augmented wave (PAW) method as implemented in VASP.[17] The Si(114) surface was represented by a six-layer slab with the theoretical equilibrium lattice constant, reconstructed on one side and passivated by hydrogen on the other, with a vacuum region of at least 10 Å. Full atomic relaxation was performed for all but the bottom silicon layer.

To model the adsorption and vibrations of isolated C_2H_4 molecules on Si(114), the underlying 2×1 reconstruction was doubled to 2×2. Molecular adsorption energies were calculated for fully relaxed configurations at several different surface binding sites. The kinetic-energy cutoff was 400 eV, and a single special *k*-point was used for all calculations. Harmonic vibrational frequencies were calculated from finite central differences. Displacements of 0.025 Å were used to construct the dynamical matrix for all degrees of freedom for the C and H atoms plus the two Si surface atoms to which the molecule was bound.

Results

Auger electron spectroscopy was used to calibrate the Si(114) surface carbon concentration with the dose of ethylene to the Si(114) surface. Figure 2 shows the initial carbon uptake curve for ethylene doses below 8 L. The carbon coverage was determined from the C(KLL)/Si(LMM) dN(E)/dE peak-to-peak ratios and normalized to the saturation dose (10 000 L) value (0.0216 ± 0.0003). We equate the saturation value with the carbon concentration for 1 monolayer (ML) of ethylene on Si(114). To further quantify the surface concentration for 1 ML

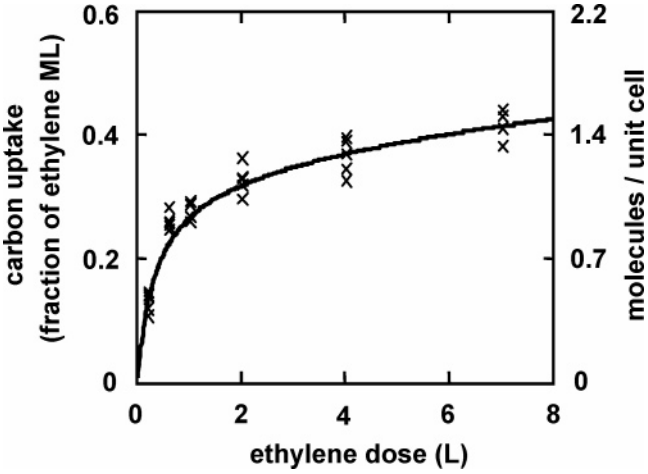

Figure 2. Initial carbon uptake curve as a measure of ethylene coverage on the Si(114) surface. Values for carbon uptake are the C(KLL)/Si(LMM) dN(E) peak-to-peak ratios normalized to the peak-to-peak ratio for saturation coverage (10 000 L dose). The approximate number of ethylene molecules per Si(114)−(2×1)/c(2×2) unit cell was determined based on saturation ethylene values for Si(100)−(2×1).

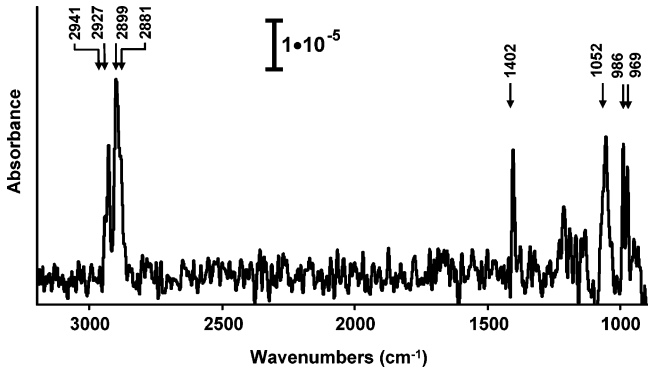

Figure 3. Transmission FTIR spectrum of a Si(114) sample with a surface coverage of 0.37 ML. The spectrum was acquired without a polarizer, using a broadband MCT-B detector and with the sample at 74° from normal incidence (Brewster's angle).

of chemisorbed ethylene on Si(114), a comparison was made with the ethylene saturated Si(001)−(2×1) surface. Auger results show the C(KLL)/Si(LMM) dN(E)/dE peak-to-peak ratio is 0.0255 ± 0.0011 on an ethylene-saturated Si(001)−(2×1) sample (10 000 L dose) in the same chamber. The ethylene saturation coverage on Si(001)−(2×1) corresponds to one ethylene molecule per dimer site, or 3.4×10^{14} ethylene molecules/cm^2, assuming a perfect surface.[1] Scaling this density by 0.848, the Si(114) to Si(001) saturation carbon coverage Auger ratio, gives an ethylene saturated surface (or 1 ML) density of 2.9×10^{14} molecules/cm^2 on Si(114). Neglecting surface defects and experimental error, this translates to about 3.6 ethylene molecules per Si(114)−(2×1) unit cell at saturation coverage. Ideally, a value of either 3 or 4 molecules per unit cell would be expected, depending on whether 1 or 2 ethylene molecules chemisorb at the tetramer site at saturation coverage. However, the value of 3.6 molecules per unit cell at saturation is used to approximate the number of molecules per unit cell versus ethylene dose in the uptake curve in Figure 2.

A transmission FTIR spectrum of chemisorbed ethylene on Si(114)−(2×1)/c(2×2) is shown in Figure 3, acquired with the sample at 74° from normal incidence (Si Brewster's angle) using unpolarized incident light and a MCT-B detector. The Si(114) substrate used for the spectrum was dosed with 4 L of ethylene, which should, according to Figure 2, result in 0.37 ML of

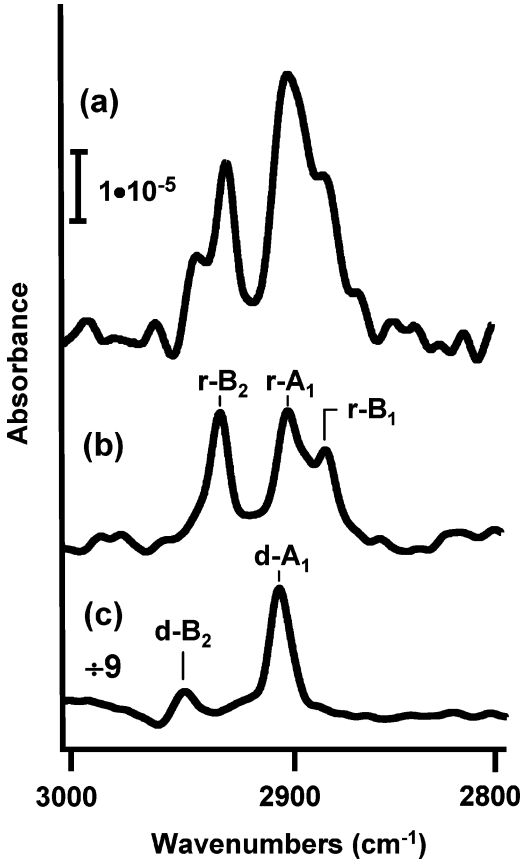

Figure 4. Comparison of C−H stretch regions for ethylene di-sigma bonded to dimers and/or rebonded atoms. (a) 0.37 ML ethylene−Si(114) (MCT-B detector); (b) 0.27 ML ethylene−Si(114); (InSb detector); (c) 0.6 ML ethylene−Si(001); (MCT-B detector). The labels identify the B_2, A_1, and B_1 C−H stretching modes for di-sigma bonded ethylene on rebonded-atom sites ("r") and dimer sites ("d").

ethylene, or about 1.3 ethylene molecules/unit cell. Eight spectral features are identified that can be positively assigned to ethylene adsorbed on Si(114). Although it appears that additional peaks may be present between 1120 and 1220 cm^{-1}, none are definitively observed above the noise level. (Note the excellent thermal stability of the system, evidenced by the absence of a derivative-shaped feature centered around 1110 cm^{-1} that occurs when small thermal fluctuations cause miscancellation of the strong silicon bulk phonon mode at that frequency.) The ethylene-Si(114) spectrum shows similarity to spectra for di-sigma bonded ethylene on other surfaces.[18−21] In, particular, the mode near 1400 cm^{-1} is often observed as a unique signature for di-sigma bonded ethylene. Ethylene is also well-known to form the di-sigma bonded structure on Si(001)−(2×1).

Figure 4 (a, b, and c) compares spectra of the C−H stretch regions for 0.37 ML ethylene-Si(114), 0.27 ML ethylene-Si(114), and 0.6 ML ethylene-Si(001)−(2×1), respectively. All spectra in Figure 4 were acquired with the sample at 74° from normal incidence. The expanded view of the C−H stretch region in the 0.37 ML ethylene-Si(114) spectrum shows the four peaks that are observed at 2941, 2927, 2899, and 2881 cm^{-1}. Three peaks are observed at 2932, 2900, and 2883 cm^{-1} for 0.27 ML ethylene coverage on Si(114) (Figure 4b), while two peaks are detected for ethylene−Si(001) at 2949 and 2906 cm^{-1} (Figure 4c). Comparison of the three spectra suggests that the 0.37 ML ethylene−Si(114) spectrum could be a combination of two slightly different structures, each of which produce the spectra observed in Figure 4b and 4c. A comparison of the correspond-

TABLE 1: Theoretical and Experimental Vibrational Frequencies for the Ethylene Molecule Adsorbed on Si(114), at the Rebonded-Atom Site and the Dimer Site

mode	C_{2v}	gas-phase parent modes[a]	theory (rebonded atom)	experiment (rebonded atom)	theory (dimer)	experiment (dimer)
asym CH stretch	B_2	ν_9	3045	2927	3059	2941
asym CH stretch	A_2	ν_5	3023	−	3040	−
sym CH stretch	A_1	ν_1	2994	∼2899− [b]	3003	∼2899+ [b]
sym CH stretch	B_1	ν_{11}	2985	2880	3001	2896
C═C + wag	A_1	ν_2, ν_7	1396	1402	1386	1402
scissor + wag	B_1	ν_{12}, ν_8	1383	−	1377	−
rock	A_2	ν_6	1192	−	1179	−
wag + scissor	B_1	ν_8, ν_{12}	1155	−	1115	−
wag + C═C	A_1	ν_7, ν_2	1100	−	1062	−
rock	B_2	ν_{10}	1052	1052	974	986, 969
scissor + C═C	A_1	ν_3, ν_2	896	−	921	−

[a] Refer to Table 2. [b] The two A_1 modes with frequencies denoted as ∼2899− and ∼2899+ are unresolved in the FTIR spectrum and appear as a single peak centered at 2899 cm^{-1} (see Figure 6). In accordance with the DFT results, the (−) and (+) signs indicate these modes are expected to be slightly below and slightly above 2899 cm^{-1}.

TABLE 2: Assignments and Vibrational Frequencies for the Gas Phase Parent Modes

mode	label	D_{2h}	C_{2v}	theory[a]	experiment[b]
asym CH stretch	ν_9	B_{2u}	B_2	3166	3106
asym CH stretch	ν_5	B_{1g}	A_2	3137	3103
sym CH stretch	ν_1	A_g	A_1	3078	3026
sym CH stretch	ν_{11}	B_{3u}	B_1	3065	2989
C═C stretch	ν_2	A_g	A_1	1640	1623
scissor	ν_{12}	B_{3u}	B_1	1423	1444
scissor	ν_3	A_g	A_1	1343	1342
rock	ν_6	B_{1g}	A_2	1199	1236
twist	ν_4	A_u	A_2	1038	1023
wag	ν_7	B_{1u}	A_1	941	949
wag	ν_8	B_{2g}	B_1	938	943
rock	ν_{10}	B_{2u}	B_2	802	826

[a] This work. [b] NIST Chemistry WebBook.

ing low-frequency modes between 900 and 1500 cm^{-1} is shown in Figure S1 (Supporting Information).

The DFT results for ethylene adsorption on Si(114) are summarized in Figure 5, which shows the equilibrium configurations for the three most favorable adsorption sites. In Figure 5a, ethylene is bridged across two rebonded atoms. Figure 5b shows ethylene chemisorbed on a dimer site and is a structure also observed for ethylene on Si(001)−(2×1) dimers.[1] Figure 5c shows ethylene bridged across the nonrebonded atoms of the tetramer site. The molecular adsorption energies at these sites are 2.41, 2.22, and 1.83 eV for (a), (b), and (c), respectively. These results are consistent with preliminary STM results (to be reported elsewhere) which indicate that initial ethylene adsorption occurs at rebonded atom and dimer sites. Accordingly, the harmonic vibrational frequencies for structures (a) and (b) in Figure 5 were calculated and are tabulated in Table 1 along with the experimental frequencies determined by transmission FTIR spectroscopy (from Figures 3 and 6). The assignments listed in Table 1 are in terms of the normal modes for gas-phase ethylene parent modes. For comparison, the harmonic vibrational frequencies for the gas-phase ethylene molecule, calculated with the same method, are listed in Table 2.

Note that the proposed structures in Figure 3 all have the ethylene C−C axis parallel to the [$\bar{1}$10] direction of the substrate. If structures 5(a) and 5(b) are, as asserted, the majority species present on the surface, then the chemisorbed ethylene will inherit the long-range structural anisotropy of the Si(114) crystal face and the orientational effects of the IR dipole selection rules should cause strong angular and polarization dependent changes in the relative peak intensities. Figure 6 shows such angular and polarization dependent spectra of the C−H stretch region collected in three different configurations at ethylene coverages of 0.37 ML. These different configurations will identify which modes have transition dipole orientations that are primarily (a) normal to the surface; (b) in the surface plane and parallel to [$\bar{1}$10]; or (c) in the surface plane and perpendicular to [$\bar{1}$10].

The spectrum in Figure 6c, for unpolarized incident light at a sample angle of 74° (Brewster's angle), is an expansion of the C−H stretch region in Figure 3. Note that when the beam impinges on the sample at this angle, the P-component is transmitted but most of the S-component is reflected. Polarization-dependent spectra, acquired at normal incidence, are shown in Figure 6b,c. The spectrum of Figure 6b was recorded with the electric field of the beam parallel to the rows on the substrate (the [$\bar{1}$10] direction), and that in Figure 6c with the field perpendicular. Dramatic differences in the relative intensities are indeed observed for these configurations, providing evidence that the ethylene monolayer is well-ordered and chemisorbed with uniformly aligned bond orientations. The calculated frequencies, scaled by a factor of 0.964, are plotted above in Figure 6.

Discussion

Based on the transmission FTIR spectrum in Figure 3, the general structure formed by chemisorption of ethylene on clean Si(114)−(2×1) at 295 K can be identified as a di-sigma bonded species. In addition to the calculated frequencies in Table 1, agreement is also found with vibrational data for known di-sigma bonded ethylene on other surfaces.[18−20] The ethylene/Si(114) peak at 1402 cm^{-1} is in excellent agreement with modes generally assigned as A_1 CH_2 scissor modes for di-sigma bonded ethylene on other surfaces. (However, the DFT results for ethylene−Si(114) indicate this A_1 mode is a combination of the A_g C−C stretch and B_{1u} C−H wagging modes for gas-phase ethylene, as indicated in Tables 1 and 2.) On Si(100), we observe this mode at 1397 cm^{-1} (for 0.4 ML coverage) by transmission FTIR, and it is reported at 1414 cm^{-1} by reflection−absorption FTIR for the Pt(111) surface. The peaks observed from 2941 to 2881 cm^{-1} and from 1052 and 969 cm^{-1} in the ethylene/Si(114) spectra are also in the expected regions for CH_2 stretching and bending modes, respectively, for di-sigma bonded ethylene. Other commonly observed ethylene adsorption states can be discounted for Si(114). For instance, an ethylidyne species is unlikely due to the absence of the strong $-CH_3$ bending mode that would appear around 1340 cm^{-1} if methyl groups were present.[20] Furthermore, there is no evidence of dissociative adsorption products, which would be expected to generate a strong Si−H stretching mode around 2100 cm^{-1}.[22]

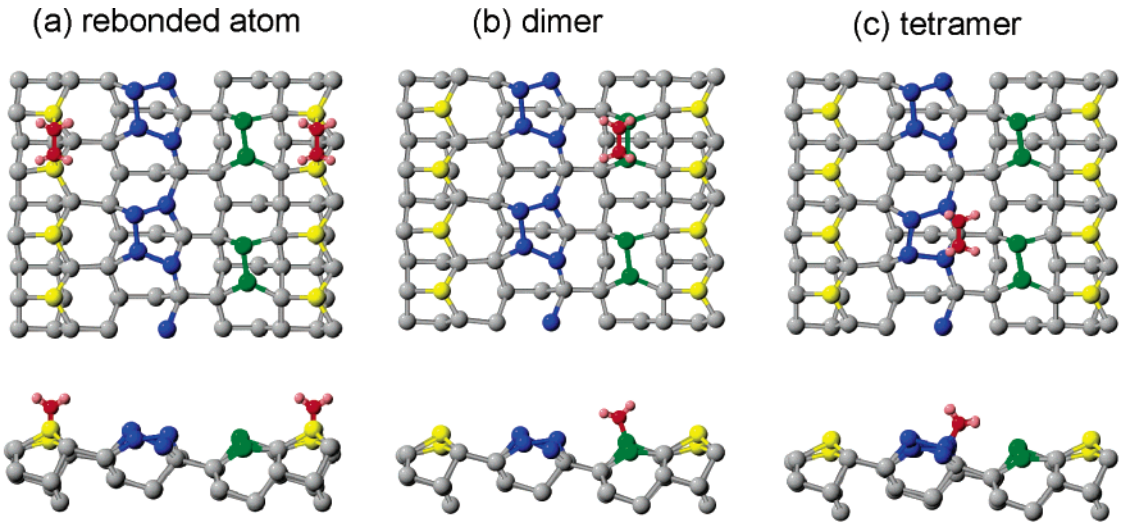

Figure 5. Top and side views of the structures determined by DFT for the three most favorable adsorption sites for ethylene on Si(114)−(2×1). The molecular adsorption energies for the equilibrium configurations shown are 2.41, 2.22, and 1.83 eV for (a), (b), and (c), respectively.

Figure 4 shows that there is a coverage dependence for the ethylene−Si(114) C−H stretching region. At 0.27 ML (Figure 4b), three peaks are observed, and at 0.37 ML (Figure 4a), four peaks are observed. Three IR-active C−H stretch modes are expected for a single di-sigma bonded ethylene structure with C_{2v} symmetry. Since Si(114) contains several types of adsorption sites, it is possible the observed coverage dependence is related to the product distributions of chemisorbed ethylene at different adsorption sites. Figure 5 shows the three most favorable structures that were identified by DFT calculations for ethylene adsorbed at the rebonded atom, dimer, and tetramer sites, with adsorption energies of 2.41, 2.22, and 1.83 eV, respectively.

To determine if separate components due to the structures in Figure 5 are present and identifiable in the ethylene−Si(114) spectra, Figure 4a and 4b are compared with a spectrum of 0.6 ML ethylene on Si(001)−(2×1) in Figure 4c. Two peaks are observed in the ethylene−Si(001) spectrum and are labeled d−B_2 and d−A_1 for the B_2 and A_1 ethylene-dimer C−H stretch modes. Assuming that ethylene on Si(001) dimers and Si(114) dimers will have similar C−H stretch frequencies, the ethylene−Si(001) spectrum can be used to identify possible ethylene-dimer peaks in the ethylene−Si(114) spectra. Comparison of the spectra show that the ethylene-dimer B_2 mode (d−B_2) observed for ethylene−Si(001) dimers is at a frequency also observed in the 0.37 ML ethylene−Si(114) spectrum (4a) but not for the 0.27 ML ethylene spectrum (4b). Thus, assuming that ethylene-dimer C−H absorption intensities are observed in the 0.37 ML ethylene−Si(114) spectrum but not in the spectrum for 0.27 ML ethylene−Si(114), the latter spectrum could possibly be due to ethylene adsorbed at the rebonded atoms (Figure 5a) or tetramers (Figure 5c). DFT calculations predict the rebonded atom structures to be lower in energy by 0.58 eV. Thus, the peaks observed in spectrum 4b are tentatively assigned to the B_2, A_1, and B_1 C−H stretch modes for ethylene-rebonded atom structures, and the peaks in spectrum 4a are assigned to a mixture of ethylene-rebonded atom and ethylene-dimer structures.

Further confirmation of these assignments is provided by the agreement between the experimental frequencies for ethylene−Si(114) and the DFT calculated frequencies for the structures in Figure 4a and 4b, shown in Table 1. The experimental C−H stretch frequencies in Table 1 are from Figure 6, while the other frequencies are from Figure 3. For both experiment and theory, the ethylene-dimer C−H stretch frequencies are higher (by up to 17 cm^{-1}) than the ethylene-rebonded atom C−H stretch frequencies. The calculated A_1 C−C + wag frequencies are at 1396 cm^{-1} (rebonded atom) and 1386 cm^{-1} (dimer), while experimentally only one peak is observed at 1402 cm^{-1}. Particularly good agreement is found for the B_2 rocking mode. Both calculated and experimental frequencies are at 1052 cm^{-1} for rebonded atom sites, and for dimer sites the calculated frequency is 974 cm^{-1}, while two peaks are observed experimentally at 986 and 969 cm^{-1}.

The ethylene/Si(114) CH stretch region can be further characterized by the angular and polarization dependence (Figure 6). The dramatic differences in relative peak intensities observed in these spectra indicate that the majority of chemisorbed ethylene on Si(114) has uniformly aligned bonds. For C_{2v} symmetry, normal modes with A_1, B_1, or B_2 irreducible representations can be IR active. Figure 7 shows the orientations of the transition dipole moments for the di-sigma bonded ethylene normal modes with these irreducible representations. By relating these transition dipole moment orientations to the structures in Figure 4, it is expected that the A_1 modes will be approximately normal to the surface, the B_1 modes parallel with the surface along the [$\bar{1}$10] direction, and the B_2 modes also parallel with the surface, but perpendicular to the [$\bar{1}$10] direction. In Figure 6, the positions of the theoretical frequencies plotted above indicate that these relative peak intensity changes should be observed for two di-sigma bonded structures, each with three IR active C−H stretch modes.

The observed changes in relative peak intensities in Figure 6 agree well with the ethylene-rebonded atom and ethylene-dimer models in Figure 5. The two peaks identified as B_2 modes for the dimer and rebonded structures are clearly resolved in Figure 6 and have the greatest relative peak intensities for normal incident light polarized perpendicular to [$\bar{1}$10] (configuration c). In Figure 6b (*E* parallel to [$\bar{1}$10]), the dimer and rebonded B_1 modes are also both resolved and have the highest relative peak intensities for this configuration. For the configuration with the sample at 74° from normal incidence, Figure 6a shows that the peak at 2899 cm^{-1} containing the two unresolved A_1 modes has the highest relative intensity. Therefore, structures 5a and 5b are strongly supported by the angular and polarization dependent spectra.

The current results show that ethylene forms highly ordered structures on Si(114)−(2×1)/c(2×2) with possible coverage-dependent product distributions; work underway verifying the

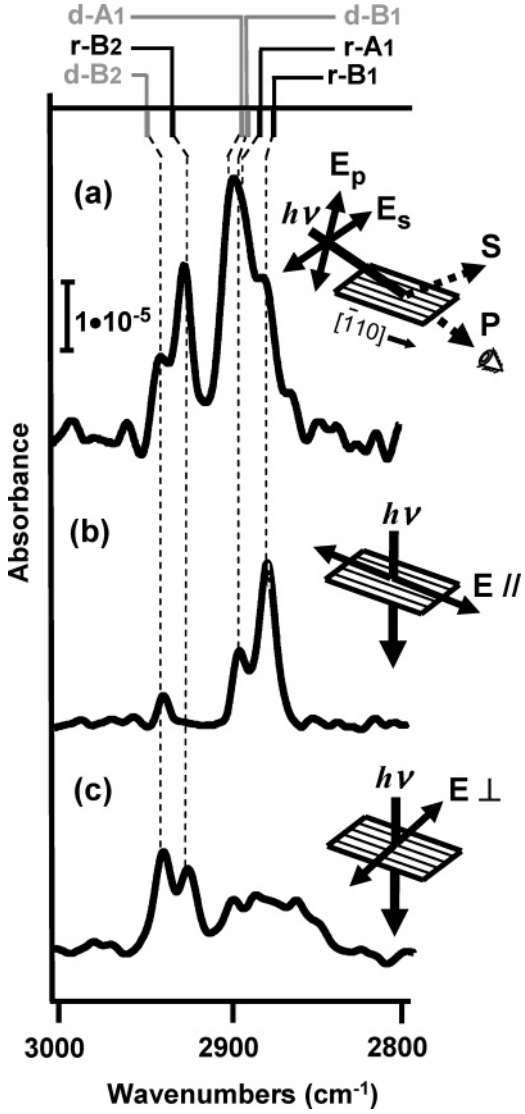

Figure 6. Angular and polarization dependent spectra for 0.37 ML ethylene on Si(114). The geometry of the sample relative to the incident beam and polarization is indicated in the side figures. (a) 74° from normal incidence; (b) normal incidence, *E* parallel to [$\bar{1}$10]; (c) normal incidence, *E* perpendicular to [$\bar{1}$10]. Positions of the calculated vibrational frequencies in Table 1 are plotted above with a 0.964 scaling factor. The labels identify the B_2, A_1, and B_1 C−H stretching modes for di-sigma bonded ethylene on rebonded atom sites (r) and dimer sites (d).

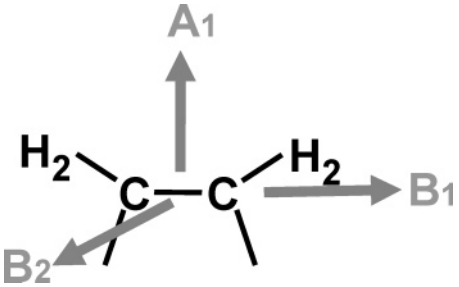

Figure 7. Transition dipole moment orientations for di-sigma bonded ethylene vibrational modes with the A_1, B_1, and B_2 irreducible representations.

actual ethylene adsorption sites with STM will help identify relationships between silicon surface structure and reactivity with organic adsorbates. Indications are that it may be possible to preferentially terminate the different Si(114) surface sites to various degrees by simple gas-phase chemisorption on the clean surface. This possibility has implications for self-assembly of organic nanostructures on silicon, as well as for elucidating relationships between organic chemisorption and silicon surface structure.

Conclusion

Ethylene chemisorbs on clean Si(114)−(2×1)/c(2×2) at 295 K to form di-sigma bonded structures. Transmission FTIR spectra of <0.4 ML ethylene-Si(114)−(2×1)/c(2×2) are consistent with DFT results, which identify the most favorable structures as bonded at the rebonded atom and dimer sites with the C−C axis parallel to the [$\bar{1}$10] direction of the Si(114)−(2×1)/c(2×2) surface. An important implication of this work is that, like the (001) surfaces of the group(IV) semiconductors, Si(114)−(2×1)/c(2×2) behaves as a "surface molecular reagent",[4] but with a unique variation of reactive sites, lattice structure, and electronic structure. Thus, this surface can play a potentially important role in elucidating relationships between surface structure and organic reaction mechanisms on Si. Si(114)−(2×1)/c(2×2) should also be a valuable substrate for self-assembled molecular nanostructure growth, with the potential to create quasi-1D structures with long-range order and alignment.

As a final note, this work shows that with proper thermal and mechanical stability, IR source, optical components, and detector, transmission FTIR spectroscopy can be used to observe the weak C−H stretching and bending modes of organic monolayers on silicon over the mid-IR range without interference from the bulk Si phonon modes. Compared with the more conventional multiple internal reflection geometry, transmission mode is a simpler experimental setup and enables both angular and polarization dependent vibrational spectroscopy on the same Si substrate, an important benefit (particularly for complex, structurally anisotropic high index surfaces). In addition, the sensitivity of such spectra to the transition dipole moment orientations of the vibrational modes, as well as the vibrational frequencies, provides sensitive experimental signatures for determining adsorbate geometries. We expect transmission FTIR will play an increasingly important role in the characterization of semiconductor surface chemistry, particularly on Si substrates.

Acknowledgment. This work was supported by the Office of Naval Research. D.E.B. was supported by an NRC/NRL Postdoctoral Research Associateship. We thank Dr. Vic Bermudez for his helpful comments and suggestions.

Supporting Information Available: Figure S1 compares transmission FTIR spectra between 900 and 1500 cm^{-1} for 0.37 ML ethylene−Si(114), 0.27 ML ethylene−Si(114), and 0.35 ML ethylene−Si(001). This information is available free of charge via the Internet at http://pubs.acs.org.

References and Notes

(1) Waltenburg, H. N.; Yates, J. T. *Chem. Rev.* **1995**, *95*, 1589.
(2) Wolkow, R. A. *Annu. Rev. Phys. Chem.* **1999**, *50*, 413.
(3) Hamers, R. J.; Coulter, S. K.; Ellison, M. D.; Hovis, J. S.; Padowitz, D. F.; Schwartz, M. P.; Greenlief, C. M.; Russell, J. N. *Acc. Chem. Res.* **2000**, *33*, 617.
(4) Filler, M. A.; Bent, S. F. *Prog. Surf. Sci.* **2003**, *73*, 1.
(5) Baski, A. A.; Erwin, S. C.; Whitman, L. J. *Surf. Sci.* **1997**, *392*, 69.
(6) Liu, H. B.; Hamers, R. J. *J. Am. Chem. Soc.* **1997**, *119*, 7593.
(7) Hamers, R. J.; Hovis, J. S.; Lee, S.; Liu, H. B.; Shan, J. *J. Phys. Chem. B* **1997**, *101*, 1489.
(8) Erwin, S. C.; Baski, A. A.; Whitman, L. J. *Phys. Rev. Lett.* **1996**, *77*, 687.

(9) Smardon, R. D.; Srivastava, G. P.; Jenkins, S. J. *Phys. Rev. B* **2004**, *69*.
(10) Laracuente, A.; Erwin, S. C.; Whitman, L. J. *Appl. Phys. Lett.* **1999**, *74*, 1397.
(11) Smardon, R. D.; Srivastava, G. P. *Surf. Sci.* **2004**, *566*, 895.
(12) Gay, S. C. A.; Srivastava, G. P. *Phys. Rev. B* **1999**, *60*, 1488.
(13) Chabal, Y. J.; Raghavachari, K. *Surf. Sci.* **2002**, *502*, 41.
(14) Nishino, H.; Yang, W.; Dohnalek, Z.; Ukraintsev, V. A.; Choyke, W. J.; Yates, J. T. *J. Vac. Sci. Technol. A* **1997**, *15*, 182.
(15) Griffiths, P. R.; de Haseth, J. A. *Fourier Transform Infrared Spectrometry*; Wiley: New York, 1986.
(16) Perdew, J. P.; Burke, K.; Ernzerhof, M. *Phys. Rev. Lett.* **1996**, *77*, 3865.
(17) Kresse, G.; Furthmüller, J. *Phys. Rev. B* **1996**, *54*, 11169.
(18) Nagao, M.; Umeyama, H.; Mukai, K.; Yamashita, Y.; Yoshinobu, J.; Akagi, K.; Tsuneyuki, S. *J. Am. Chem. Soc.* **2004**, *126*, 9922.
(19) Lal, P.; Teplyakov, A. V.; Noah, Y.; Kong, M. J.; Wang, G. T.; Bent, S. F. *J. Chem. Phys.* **1999**, *110*, 10545.
(20) Fan, J. F.; Trenary, M. *Langmuir* **1994**, *10*, 3649.
(21) Widdra, W.; Huang, C.; Yi, S. I.; Weinberg, W. H. *J. Chem. Phys.* **1996**, *105*, 5605.
(22) Chabal, Y. J.; Raghavachari, K. *Phys. Rev. Lett.* **1984**, *53*, 282.